Int J Adv Manuf Technol (2014) 75:991–1003
DOI 10.1007/s00170-014-6113-z

ORIGINAL ARTICLE

Study on analysis and prediction of riveting assembly variation of aircraft fuselage panel

Gang Liu · Honglun Huan · Yinglin Ke

Received: 7 January 2014 / Accepted: 25 June 2014 / Published online: 8 August 2014

Abstract This investigation is performed to develop a methodology for the variation analysis and prediction of aircraft fuselage panel riveting assembly. Firstly, according to the manufacturing process of the part of the aircraft fuselage panel, the method of influence coefficient (MIC) based on key feature deviation is proposed. Secondly, the mechanism of component deformation in riveting process is expounded, and the method to approximately compute the global distortion, caused by rivet deformation, of the fuselage panel is presented. The proposed method is illustrated through a case study on the riveting assembly process of a sidewall panel, the local plastic deformation near the riveting holes is ignored but the computing resources are saved, the complex and time-consuming computation are avoided. The reasonableness of the proposed method is verified by the measurement data of the prototypes.

Keyword Aircraft fuselage panel · Riveting assembly variation · Finite element method · Method of influence coefficient (MIC) · Monte Carlo method

1 Introduction

How to predict the assembly variation and then allocate the tolerance and the coordination of the parts have been a major challenge in many industries, especially in the areas that weak stiffness sheet metal parts are widespreadly used, such as aerospace and automotive industries. Assembly variation reduces the accuracy of the product, impairs the assurance of the coordination, propagates and directly impacts on the subsequent process, and ultimately lowers the overall product quality. And more, forced assembly stress is introduced following the assembly variation and continuously acting on the parts and then increases the average stress and finally reduces the anti-fatigue or withstanding stress corrosion capacity. According to the statistics, there is 65–70 % of design changing or failure is caused by the inaccurate prediction of the dimension or geometric size [1].

By means of accurate variation analysis and predication, one can optimize the design and the tolerance distribution of the sheet metal parts and also can configure the fixture tooling, evaluate the assembly process, plan on anti-deformation, and so on ahead of schedule.

Since the 1990s, assembly variation analysis and prediction of flexible parts has been developed and used in the automotive and aerospace industries. There are three variation analysis methods most widely used: worst-case approach, root sum squares (RMS), and Monte Carlo simulation [2]. Huang et al. divided the variation source into three types as follows: fixture deviation, part variation, and the assembly sequence [3, 4]. Liu et al. proposed a general method known as the method of influence coefficient (MIC) [5]. The method divided the assembly process into the following four steps: location, clamping, fastening, and releasing. The force and the displacement in each step were analyzed, and finally, the relationship between the variation of the parts and the assembly was approximated by linearization and linked by the sensitivity matrix obtained from running two times finite element analysis. Later, Cai et al. analyzed the non-linear frictional contact interaction and presented some relevant algorithm based on the MIC [6–10].

In recent years, MIC has been widely studied and applied in many aspects such as the fixture planning and design [11, 12], layout optimization and evaluation [13, 14], variation source identification [15], product-oriented sensitivity

G. Liu · H. Huan (✉) · Y. Ke
The State Key Lab of Fluid Power Transmission and Control, Zhejiang University, Hangzhou 310027, China
e-mail: honunhuan@gmail.com

analysis of variation feature of parts and assembly station [16], and etc.

Because of the continuity of the surface, the variations between different points always have some relevance. Merkley measured the relevance by the geometry covariance [17]. Camelio studied how to identify the deviation feature of compliant parts from measurement data based on the geometry covariance and the MIC, PCA (principle component analysis) methods [18]. Cai et al. studied the relationship between assembly variation, expressed as translational and orientational variations at certain key product/process characteristic points (KPCs), and workpiece surface errors (part variations), fixture set-up errors (locating variations). In order to minimize the assembly variation, the authors proposed and verified "N-2-1" locating principle for deformable sheet metal parts as compared to "3-2-1" principle. And also, they developed some approaches and introduced the simulation packages by the numbers for optimal sheet metal fixture design [19–21].

For the assembly variation caused by the joints, Cai et al. studied the influence on the dimensional variation of the assembly which connected with the self-piercing riveting (SPR) and the spot welding process [22]. They analyzed and predicted the aluminum alloy sheet metal assembly variation and considered that the variation produced by the self-piercing riveting was an important factor. Moos Sandro et al. studied the local plastic deformation caused by resistance spot welding and integrated the result into the model of tolerance analysis of sheet metal assembly [23]. In [24], it was also shown that mechanical joining techniques cause distortion or variation significantly in joined assemblies and influence the assembly quality.

However, earlier researches on the assembly variation analysis generally take the variation of the parts, the tools and the local deformation, the assembly sequence, and etc. into account. For the fuselage assembly, the manufacturing process and the connection between the parts all have its own peculiarity.

Firstly, aircraft fuselage panels are usually composed of the sheet metal parts such as skins, frames, stringers, and corners which are joined by a huge number of solid rivets. Most of the parts are obtained by the manufacturing process of knee bending or roll bending. Special phenomenon such as spring back and distortion cause the random bias of the key feature, existing between the actual parts and the ideal ones. Secondly, the riveting process includes seriously non-linearity such as the material, the geometry, and the contact interaction. The riveting holes are squeezed non-uniformly by upsetted rivets, and so, plastic deformation not only occurs on the rivets but also around the corresponding holes. The number of the rivets is so large that causes the panel bending along the riveting seam and then the global distortion. Although with the advancement of the software and the hardware technology, numerical simulation based on finite element method has greatly improved, it is still very difficultly to simulate the

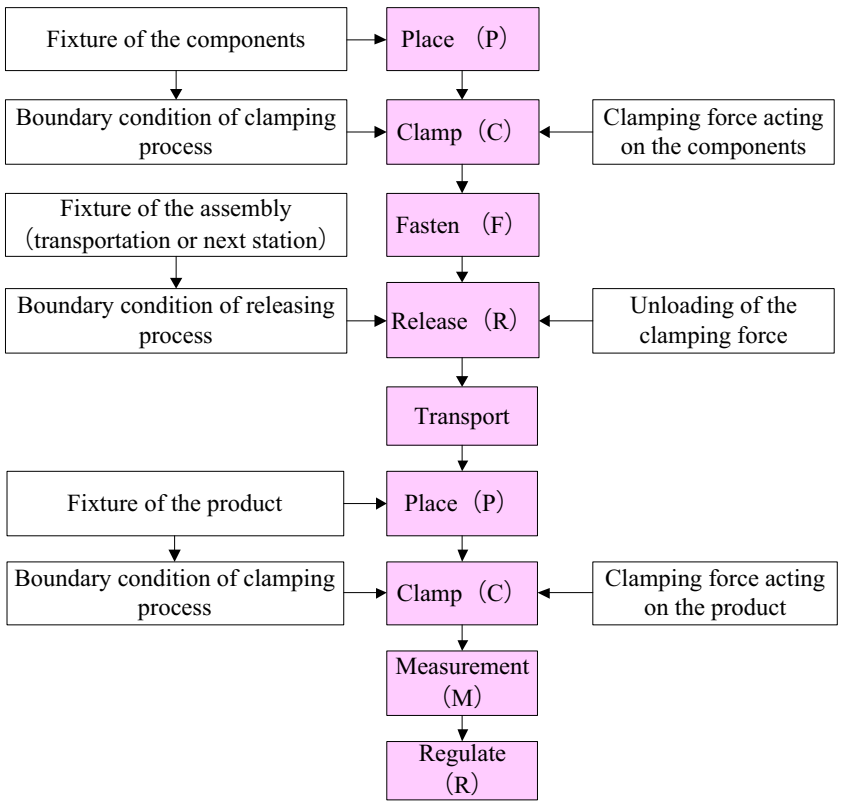

Fig. 1 Illustration of assembly process

riveting process that includes thousands of rivets and holes with elastic-plastic deformation directly.

This investigation is developed mainly to overcome the aforementioned problems. In Section 2, the details about the riveting assembly process of the fuselage panel and the variation sources are elaborated. In Section 3, the methodology for analyzing and predicting the variation with balancing the precision, the efficient, and the computation resource is given. In more detail, the MIC based on feature deviation is proposed in Section 3.1, the riveting deformation mechanism of the solid rivets and the riveting holes is analyzed and the model is created hereafter, the method to take the riveting deformation into account in the variation analysis is presented and verified by a finite element analysis model in Section 3.2. Section 4 outlines a case study of a side panel assembly process. Section 5 draws the conclusion.

2 Riveting assembly process of the aircraft panel

Usually, aircraft panel is assembled on a special type of frame and experiences the classical PCFR (place, clamp, fasten, and release) cycle, proposed also in [25]. After assembly, the product will be transported to the next station and also experience the PCMR (place, clamp, measure and regulation) cycle, analogous with the PCFR. In the process, there are not only the clamping loading and unloading, deformation of the parts, and the product but also the transformation of the different boundary conditions. Its details are illustrated in Fig. 1.

The principle of the location of the parts of the aircraft panel assembly is similar with the general mechanical machining. Six freedoms are constrained in the fixture through the fitting relationship between the locators and the components. The fixtures are specifically designed, precision manufactured, and provided with good rigidity and high accuracy. Assembling usually starts after repeated measurement and adjustment. Based on these points, it is reasonable to assume that the fixture variations can be ignored and the non-ideal parts or components deform to the ideal shape under the restriction of the clamping force in the positioning and the clamping steps.

The fasteners in the aircraft panel mostly are solid rivets. The shank is hammered by a pneumatic riveting gun or squeezed by automotive riveting machine and then the rivet hole is expanded, the workpieces elongated, or bent along the riveting seams. After being riveted, components break away the restriction and are carried to a new station by a conveyance or constrained by new fixtures. Each of them has a tendency to recover to the original shape. Inner force in the product has been produced and acts at the riveting points. Some components recover closely to the initial state, and some come into being newly deformed under the force.

And more, because of the flexibility of the panel, it shows different shapes under different supporting or clamping modes due to gravity, and the measurement results are different too. As shown in Fig. 2, assembly of an aircraft side panel is accomplished on a special frame by manual or automated riveting device. After transportation and panel joint installation, it will be integrated with other panels to form a fuselage section. Before the integration, measurement and evaluation are required, and the panel is supported by a group of three axis positioner on this status, which satisfies the n-2-1 placing method.

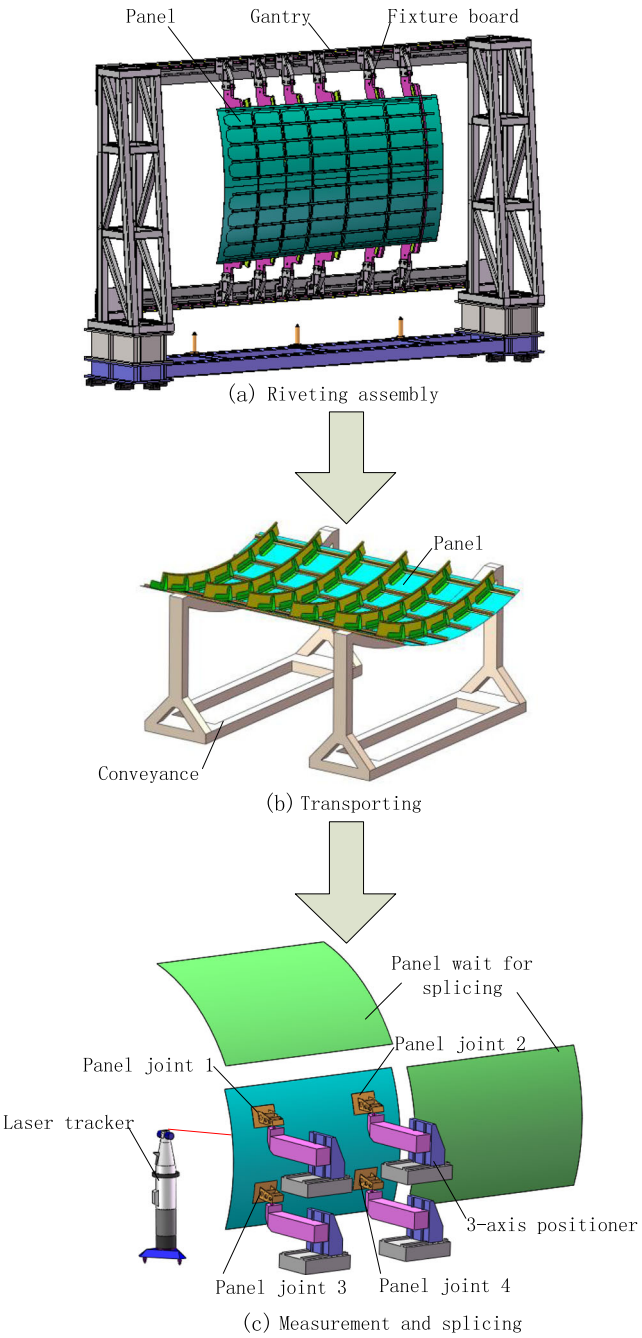

Fig. 2 Panel assembly and transportation between the stations

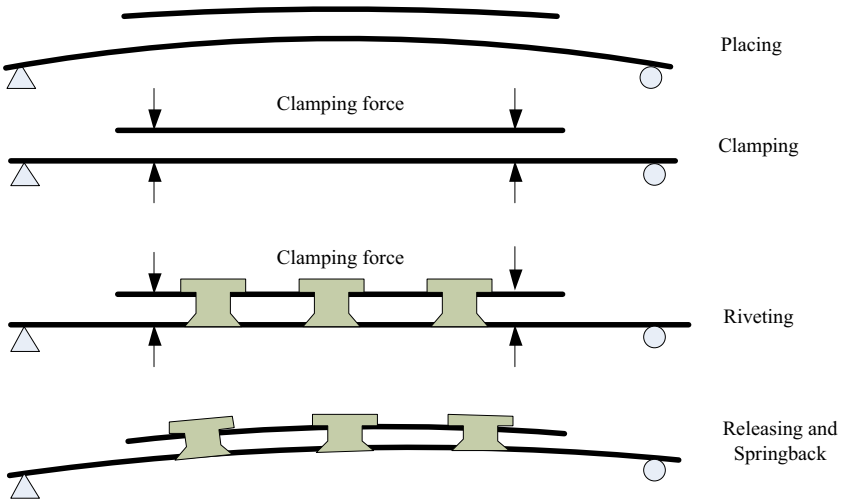

Fig. 3 Parts' deviation propagation in assembly process

3 Calculation of the assembly variation

From the above discussion, there are mainly three sources causing the assembly variation: part deviation, riveting deformation, and the locating method at measurement state. Assuming that product variation caused by deviation of the parts is $\boldsymbol{X}^{\mathrm{C}}$, by riveting deformation is $\boldsymbol{X}^{\mathrm{R}}$, and by gravity is $\boldsymbol{X}^{\mathrm{G}}$. Ignored the coupling between the variation source of different factors, the total variation X can be obtained

$$\boldsymbol{X} = \boldsymbol{X}^{\mathrm{C}} + \boldsymbol{X}^{\mathrm{R}} + \boldsymbol{X}^{\mathrm{G}} \tag{1}$$

As well known, $\boldsymbol{X}^{\mathrm{G}}$ can be calculated by the finite element method directly. So, we only give the method to calculate $\boldsymbol{X}^{\mathrm{C}}$ and $\boldsymbol{X}^{\mathrm{R}}$ below, respectively.

3.1 Assembly variation caused by part deviation

For most sheet metal parts, dimensional problem is mainly caused by deformation on the normal direction of the surface. Figure 3 shows the PCFR cycle of the assembly variation generated only by part deviation.

Camelio proposed the method of influence coefficient to analyze the variation of assembling process [26]. According to the characteristics of the manufacturing of the sheet metal parts of the aircraft, spring back and twisted warped distortion are main obstacles to obtain an accurate geometry size and shape. Accordingly, the bending and torsion angles become the key characteristics for describing the accuracy of the size and shape. The elementary geometry shows that when bending angle or torsion angle deviation is small, the influent relationship between the deviation of parts and product could be considered as linear. Therefore, the MIC based on the key characteristics of the parts could be proposed.

Similarly, with the MIC based on point deviation, assume that the variation of key characteristic i of the parts is α_i, impact on the variation X_k of the measurement point M_k is s_{ik}. That is to say,

$$X_k = s_{ik}\alpha_i \tag{2}$$

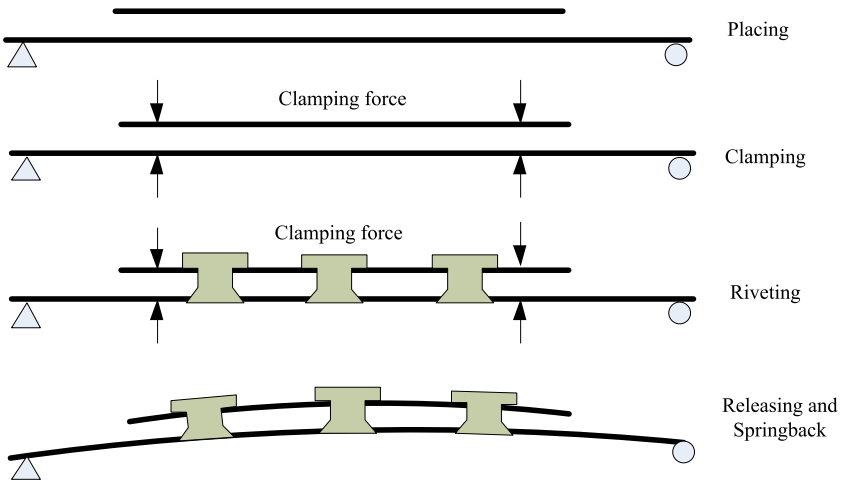

Fig. 4 Riveting deformation in assembly process

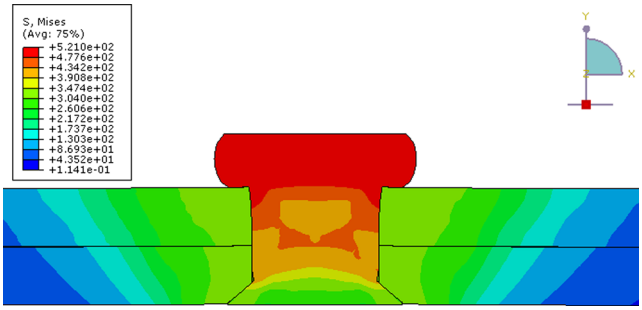

Fig. 5 Stress distribution in the riveted components

The matrix format is

$$\boldsymbol{X}^{\mathrm{C}} = \begin{pmatrix} X_1 \\ \vdots \\ X_M \end{pmatrix} = \begin{pmatrix} s_{11} & \cdots & s_{1N} \\ \vdots & \cdots & \vdots \\ s_{M1} & \cdots & s_{MN} \end{pmatrix} \begin{pmatrix} \alpha_1 \\ \vdots \\ \alpha_N \end{pmatrix} \tag{3}$$

Simply noted as $\boldsymbol{X}^{\mathrm{C}} = \boldsymbol{S\alpha}$

Usually, the probability density function of the variation of the key characteristics could be obtained by experience or statistics. Combine the method of influence coefficient and Monte Carlo method, the probability density function of the variation of the assembly could easily be obtained.

3.2 Assembly variation caused by riveting deformation

While the riveting carries out not only the deviation of the parts but also the deformation caused by riveting deformation, the impact on the variation of the product is significant. Figure 4 illustrates the assembly variation generating process due to the riveting deformation.

Elastic-plastic deformation of the rivets and distribution of the residual stress or the strain have been studied by many researchers in the last few years [27–32]. Figure 5 shows a stress field of a 7050-T3 aluminum rivet with 5-mm diameter, 13-mm height, and two 7050-T7451 sheets with a hole with a diameter of 5.15 mm after riveting with quasi-static squeezing method analyzed by finite element software ABAQUS 6.10 [33]. Figure 6 shows the expansion of the hole after being riveted. Properties for the materials provided in ABAQUS/Explicit are shown in Fig. 7.

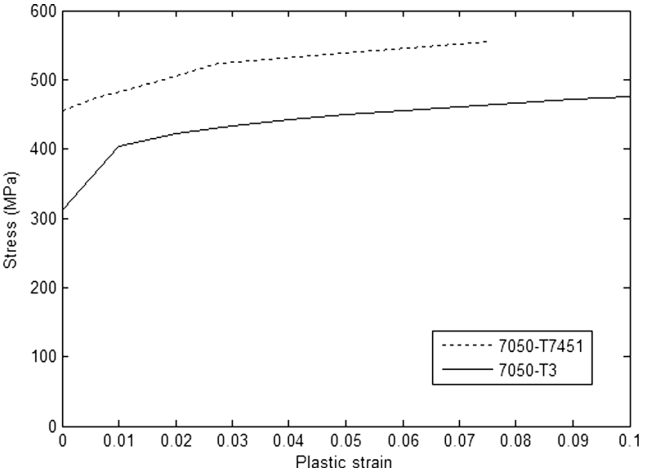

Fig. 7 Stress strain relation of the rivet and sheet materials

As seen in Fig. 6, the compressive stress through the sheet thickness is significantly uniformless due to the expansion of the rivet and the resulting interference of the upsetting side is 1 % greater than the other side. According to [27, 34, 35] the average of the sufficient interference of the riveted hole is 2 to 3.5 % and varies between 1.5 and 4 %. So, the uniformless expansion of the wall of the hole becomes the main factor of the deformation of the workpieces.

Thick-wall cylinder theory [36] can be used to approximately interpret the behavior that the riveting holes' wall is squeezed by the upsetting rivet shank. The deformation can be divided into twofold: the

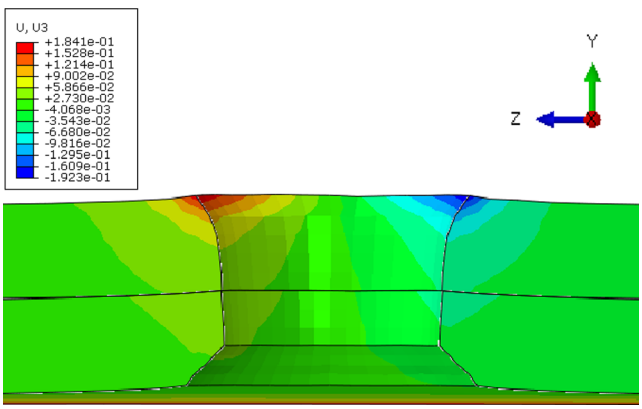

Fig. 6 Displacement distribution near the riveting hole (with scale factor 5)

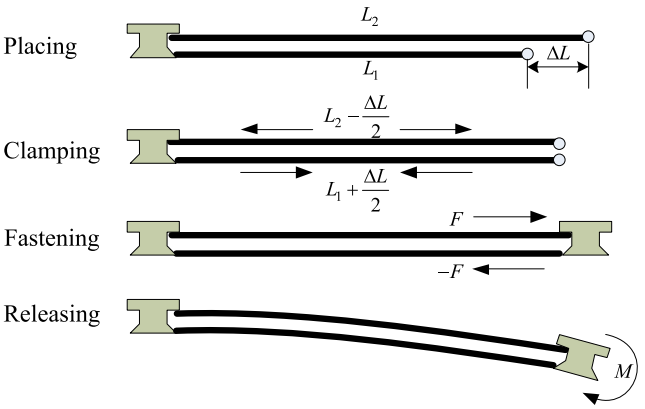

Fig. 8 Mechanism of riveting deformation and equivalent moment loading

elastic-plastic deformation near the riveting hole wall and the net elastic deformation far away from the wall. Relative to the assembly process, the greater concern is the global deformation of the product rather than the local elastic-plastic deformation. Difficulty of directly simulating the riveting assembly process, using the finite element method, also lies on non-linear interaction between the rivet and the hole, the non-linear materials, the non-linear geometry, and the huge number of rivets. For reducing the difficulty and enhancing the practicability of the finite element simulation, we ignore the local elastic-plastic deformation near the wall, and the global deformation is seen as being caused by the bending moment.

Figure 8 illustrates the mechanism of the deformation of the workpieces caused by the expansion of the rivet through the sheet thickness. Assuming that the diameter of the rivet is d, the thickness of each sheet is t, the interference of the upsetting side is δ_d, and the other side is δ_h, the difference of the interference is $\Delta\delta$; we can calculate the difference along the riveted seam between the two sheets ΔL,

$$\Delta L = \frac{d}{2}\Delta\delta.$$

Here, we define a parameter, the width of the riveting seam w, which is not quantified obviously but does not impact on the derivation or the result. Then, the area of the seam section could be written as $A=2wt$. The magnitude of the stress in the sheet is

$$\sigma = \frac{F}{A} = \frac{E\Delta L}{2} \tag{5}$$

Ignoring the local plastic deformation around the holes, deformation of the workpieces can be seen as meeting with a load of bending moment M at the ends of the seam,

$$M = Ft = \frac{EAt(L_2 - L_1)}{2} = \frac{EAt\Delta L}{2} \tag{6}$$

In the finite element simulation, due to the existence of the meshes, the ends of the seam are composed by some nodes. So, the moment loaded at the end points of the seam should be expressed as

$$p = \frac{M}{A} = \frac{Et\Delta L}{2} \tag{7}$$

The deformation of the workpieces caused by riveting not only associates with the geometry size of the rivet and the parameters of riveting process but also with the riveting sequence. We ignore the influence of the riveting sequence and assume that all the geometry size and the riveting parameters are the same for the same type of rivets. Thus, complex and excessive elastic-plastic deformation of the rivets can be simplified to few

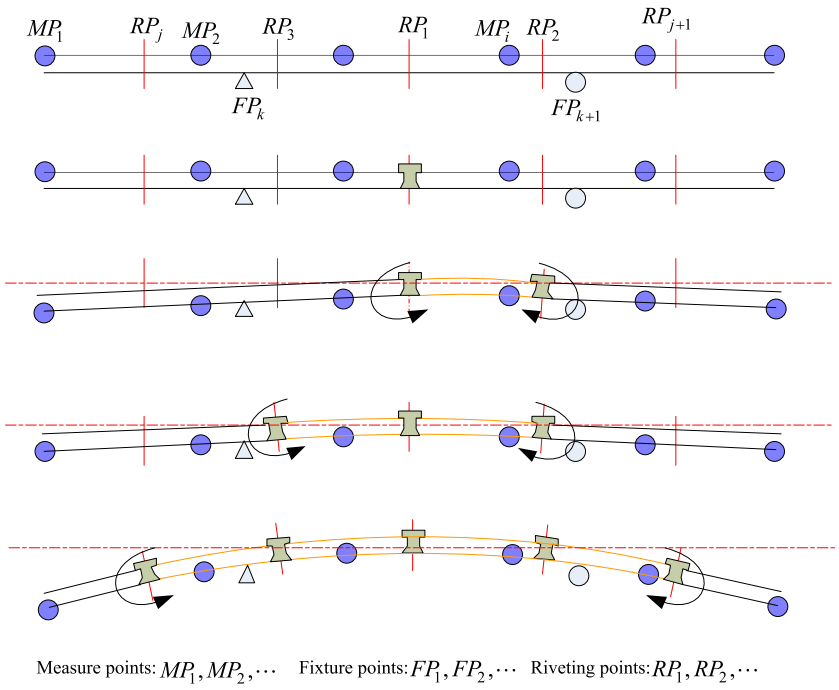

Fig. 9 Riveting deformation of multi rivets and equivalent moment loading

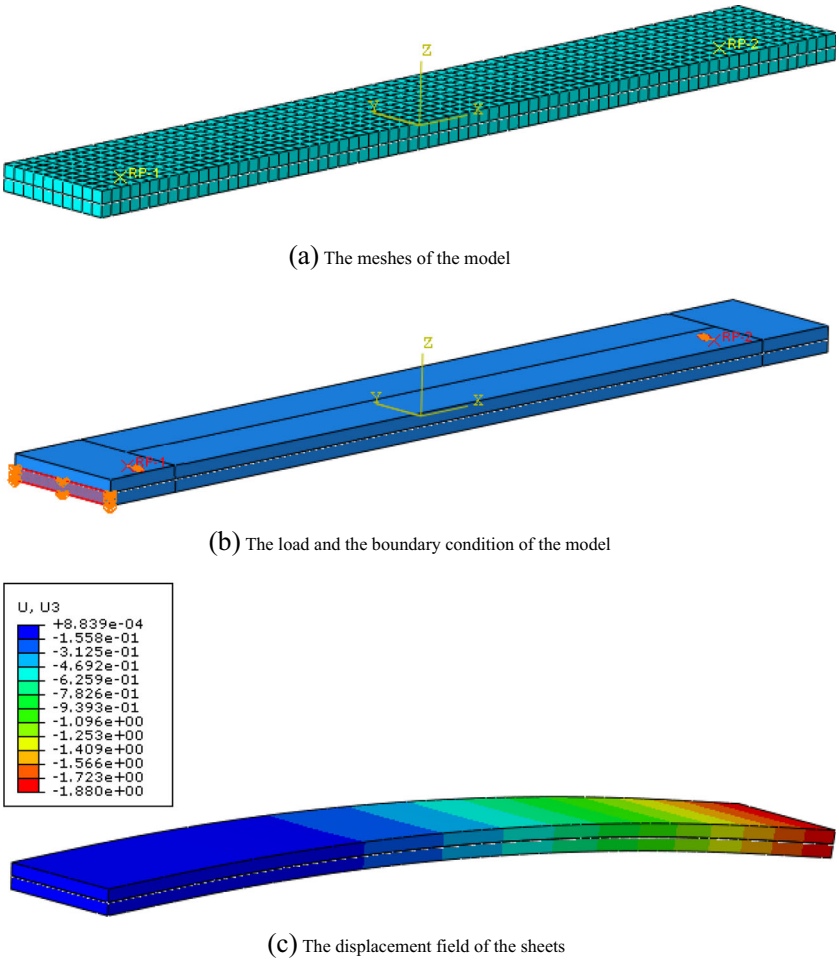

(a) The meshes of the model

(b) The load and the boundary condition of the model

(c) The displacement field of the sheets

Fig. 10 FEA model of the moment loading process. **a** The meshes of the model. **b** The load and the boundary condition of the model. **c** The displacement field of the sheets

loadings of bending moment, as shown in Fig. 9. Finally, with utilizing this method, the feasibility and practicality of the prediction of the deformation could be enhanced.

In order to validate the feasibility of the method described above, a three-dimensional finite element model is developed to simulate the effects of moment loading on the deformation utilizing the finite element software

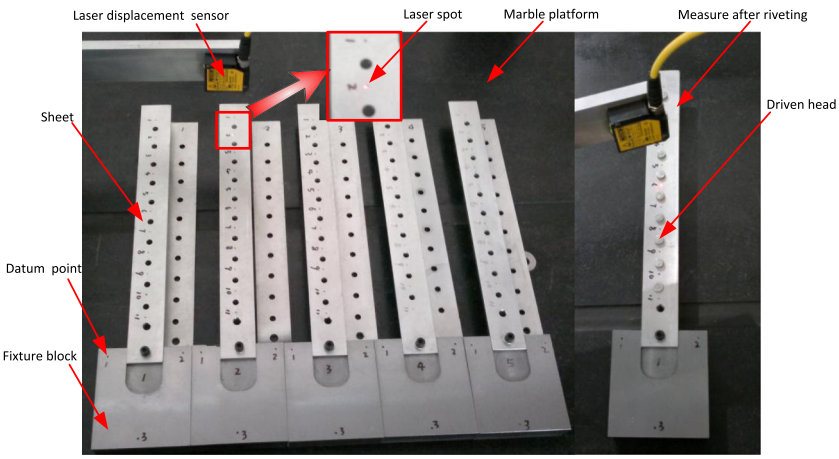

Fig. 11 Measurement of the sheets before and after riveting

ABAQUS/Standard and then the result is compared with a specialized experiment.

A configuration consisting of two 220 mm×30 mm×2.5 mm of sheets is chosen for the finite element model. The sheets are meshed using eight-node single-point integration brick elements (C3D8R), as shown in Fig. 9a. Power law plasticity models are used to describe the non-linear material behavior for the sheets. The properties used in the model are also shown in Fig. 7. Contact is implemented into the simulation using TIE options in ABAQUS/CAE. All the degrees of freedom of the end face of the below sheet are constrained as the boundary condition. The moment is loaded at the two end points of the riveting seam, with a magnitude of 2,858 which is obtained from direct computation through the formula (6), see Fig. 9b. The displacement field result of the finite element analysis is shown in Fig. 10c.

There are five pairs of 7050-T7451 sheets adopted for the experiment. The configuration chosen of each pair consisted of one with a geometry size of 270 mm×30 mm×2.5 mm and the other 220 mm×30 mm×2.5 mm. For the convenience of measurement, the longer sheet is fixed on a polished steel block. The two plates are joined at the middle line by ten 7050-T73 rivets with 5.0-mm diameter, 11-mm height, 0.94-mm depth 100°countersunk. Installation of the rivets is executed using a squeezing machine. All the height of the driven rivet heads are controlled at 3 mm. The measurement is conducted using a laser displacement sensor fixed by a jig. As shown in Fig. 11, the middle points of each two holes on the longer sheets along the riveting seam are measured twice to represent the shape of the sheets, before and after riveting, respectively. The difference of the two-time measurement is considered as the riveting deformation.

The results according to finite element simulation and experimental method are shown in Fig. 12. It is shown that the deformation on the normal direction is significantly close to each other and the difference was tolerable in the scale according to the sheet geometry size. This result indicates that the developed method can be used for riveting assembly variation analysis.

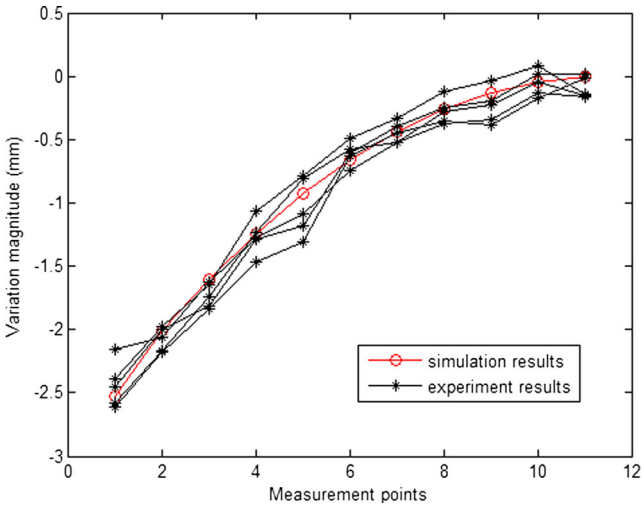

Fig. 12 Comparison of FE and experimental results

4 Case study

4.1 Constructional solutions of the fuselage panel structure

A fuselage panel of a contemporary transport aircraft prototype, as shown in Fig. 13, is studied in this section. The panel is skin structure supported by six frames and six stringers, as shown in Fig. 14. The *Z*-shaped cross-section stringers are joined by countersunk rivets directly to the skin. The frames are also *Z*-shaped cross section but joined to the clips by protrude rivets. Then, the 30 clips are joined by countersunk rivets to the skin, in order to connect the skin with the frames.

All the sheet metal parts of the panel have a thickness of 2.5 mm with the 7050 aluminum alloy except the skin YL12. The skin is a cylinder surface with a diameter of 5,400 mm, course length of 3,000 mm, and width of 2,000 mm. The distance of the frame from its neighbor is 500 mm, and for the stringer is 400 mm. There are 20, 14, 2 rivets in the joints of each clip and the skin, the frame, and the stringer, respectively, as shown in Fig. 15. Furthermore, there also are 200 rivets in joint of each stringer and the skin. Totally, the number of the countersunk rivets in the

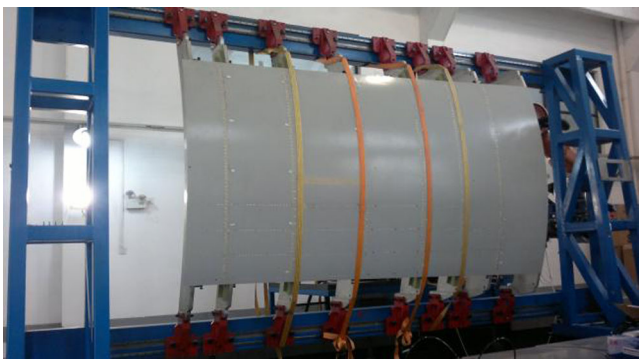

Fig. 13 A panel of a prototype aircraft

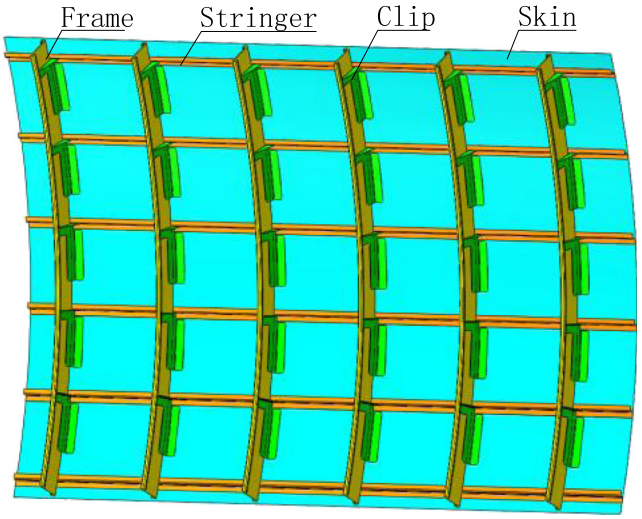

Fig. 14 Components of the panel structure

panel is 1,800 and the protrude 480. Obviously, the number of rivets is so huge that it is difficult to directly complete the finite element analysis of the plastic deformation which contains non-linear material, non-linear geometry, and non-linear boundary condition.

4.2 Variation analysis for panel assembly

Smoothly splicing with other panels is the objective of panel assembly which should be achieved. This requires that the assembly variation must be in the allowable range. Concretely, the position of the frames and the stringers must be correct and accurate, the siding surface of the frame or the stringer should be parallel with others and perpendicular to the inner surface of the skin.

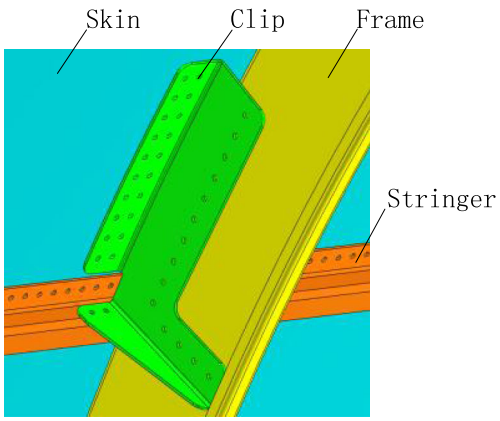

Fig. 15 Layout of the riveting joints of the panel

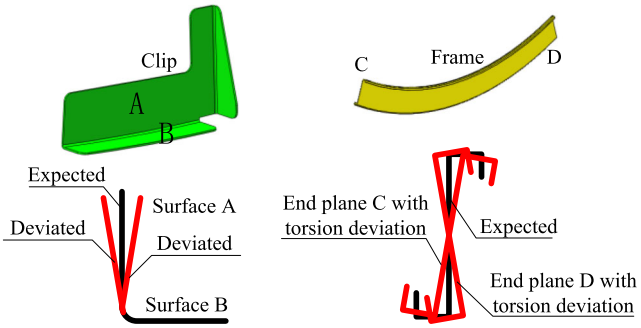

Fig. 16 Key characteristic of clip and frame and the deviation

Theoretically, deviation of each characteristic of each part could cause assembly variation. As an example, we only consider the product variation caused by the deviation of the flange angle (between the surfaces A and B) of the clips and the torsion angle of the frame (between the surfaces C and D), as shown in Fig. 16. Therefore, there are 36 key characters of all the parts.

For the panel, the key product characteristics contain the position and the direction of the frame, the position of the stringers, and the shape of the skin. Therefore, there are a total of 51 measurement points, where there are nine on the skin, five on each frame, and two on each stringer. Layout of the points (the red dots) and the mesh of the panel are shown in Fig. 17. Four points (MP1, MP2, MP3, MP4) are selected as the instance to carry out the comparison later between the simulation results and the factory data.

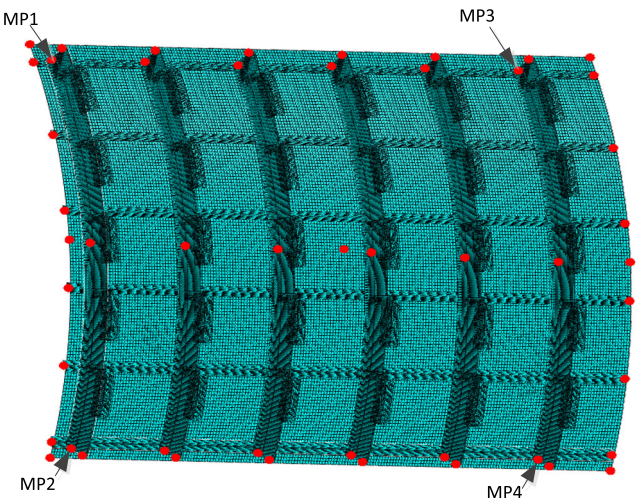

Fig. 17 FEM mesh and the measurement points of the panel

By using the method of influence coefficient based on the key characteristic, we get the influence matrix with 51 rows and 36 columns from the following steps.

(1) Modeling the variational parts

Two methods can be applied. First, the parts can be obtained through CAD software, such as SOLIDWORKS, CATIA, etc., directly. Second, based on morphing mesh approach to generate the parts with variation [37], for example in CAE software ABAQUS, it can be realized through secondary development with python language.

(2) Positioning of the variational parts

Generally, mating surfaces between the ideal parts has the same shape and could keep close to each other in the correct position. While the parts have variation, that fit does not maintain anymore, for example, the variational surface A1 (or A2, within another deviation direction, similarly to D1 and D2) and the side surface of the frame or the surface B and the inner surface of the skin. At this rate, we can choose one pair of mating surfaces (as shown in Fig. 18a, surface B and the inner surface of the skin) to keep close to each other and locate the parts with combining with other positioning methods in the assembly coordinate system. The torsional bending parts can be treated similarly, as shown in Fig. 18b.

(3) FEA of the clamping process of the variational parts

If the variation of the parts is regular, it is easy to simulate the process by finite element method, the rigid tool compacts the variational parts to the ideal shape and make the mating surface close to each other. Here, the boundary

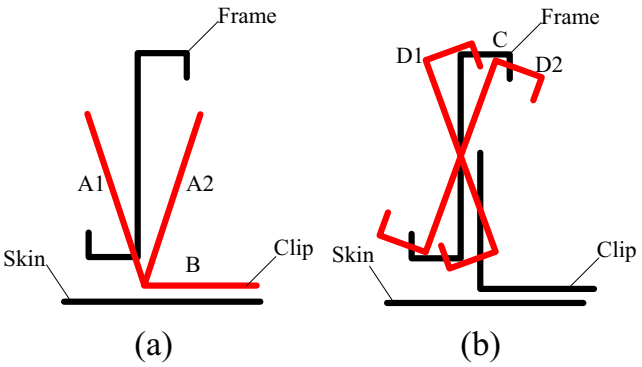

Fig. 18 Positioning of the variational parts

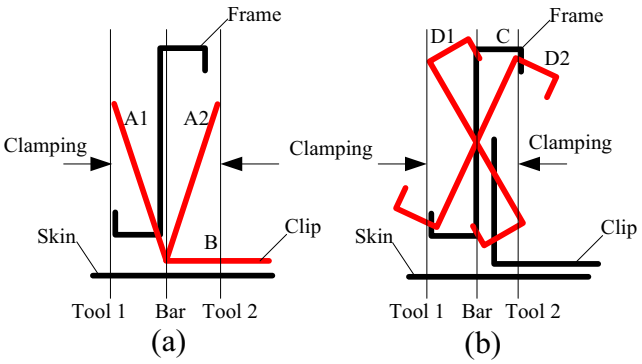

Fig. 19 Clamping of variational part

conditions are the restriction on the locating surfaces or points and keep the rigid bar fixed, and the load is the displacement of the tool from the original position to the bar, as shown in Fig. 19.

(4) Modeling the riveting joint

Based on the result of step (3), without considering plastic riveting process, we can use fasteners to model a point-to-point connection between two faces as shown in Fig. 20. This can be easily achieved in the CAE software ABAQUS through creating point-based fasteners in the interaction module [33].

(5) Modeling the spring back

In this step, after deactivating the displacement of the tool in step 3, there will be inner force in the product acting on each other through the mating surface and riveting points. The variational parts will spring back to original shape, and the others will have a new deformation. Set the boundary condition according to the measurement status, i.e., restrict the freedom of the holding area or points.

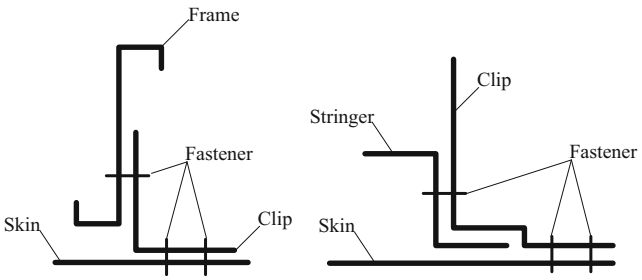

Fig. 20 Model of the riveted joint

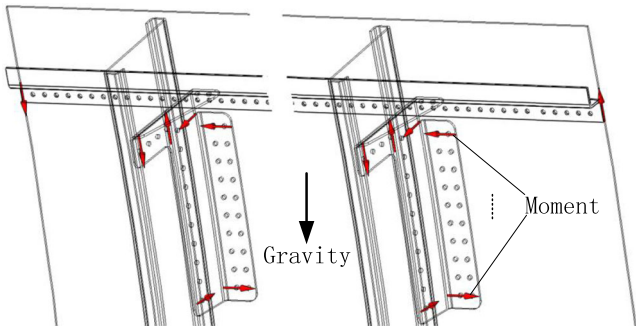

Fig. 21 Equivalent moment of riveting deformation and gravity loading on the panel

(6) Influence matrix

The variation of the measurement points of the panel can be obtained from the unit deviation of the different features of different parts. Assembling the sensitivity matrix, S can be obtained.

Based on the above discussion, the equivalent moment of riveting deformation and gravity loadings on the panel are depicted in Fig. 21. The places to load the moment are the node sets where elements come from the riveting points.

5 Result and discussion

After being riveted, the panel was measured before splicing with other panels. Figure 22 shows the deformation along the z coordinate direction of the panel due to the riveting process and the gravity. Here, the panel was supported by three positioners (deactivate the 2nd positioners in Fig. 4) with spheric hinge. It can be seen that the panel became warped with a certain distortion.

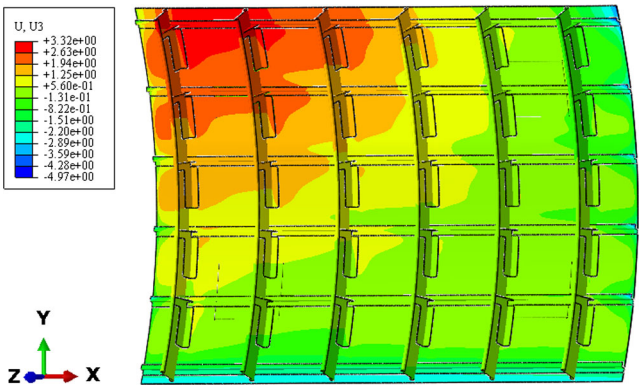

Fig. 22 Displacement U3 distribution of the panel supported by three positioners

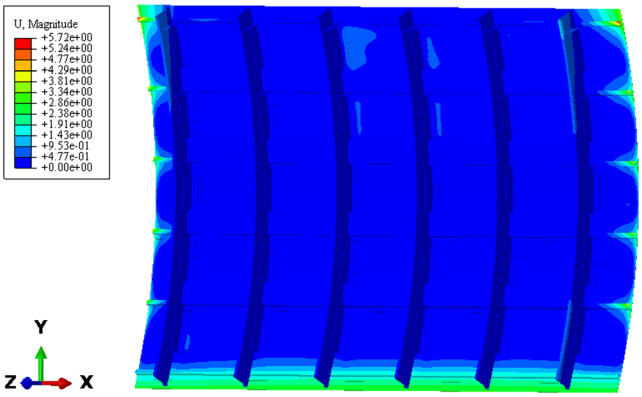

Fig. 23 Deformation of the panel supported by four positioners

Figure 23 depicts the deformation of the panel which is supported by four positioners. Although two figures depict the different variations, it still can be seen that the panel has an obviously better situation than the status supported by three positioners. It is also showed that the stiffness of the lower edge of the panel is the weakest area, which should be enhanced.

Then, by Monte Carlo method, generating the random deviation of the parts, and multiple S, the variation of the assembly can be finally obtained. According to the formula (7), we get the total variation of the product. Attributed to the CAE software ABAQUS, its secondary development with python language and MATLAB (www.mathworks.com), the efficiency of the analysis can be improved significantly.

According to statistics, the mean of the deviation of the clip angle is 0 and the variation 3° and the mean of the deviation of the frame angle is 0 and the variation 5°. By finite element analysis and MATLAB computation, we obtain the prediction results about the leftmost frame and comprised them with two factory data which are measured by laser tracker, details are shown in Table 1 and the distribution histogram is shown in Fig. 24. As seen from the comparison, the prediction and the factory data are very consistent. The effectiveness of the proposed method is well illustrated.

Table 1 Comparison of prediction and factory data

	Mean	Variance	Factory data 1	Factory data 2
MP1	1.0703	20.4784	1.0129	0.9581
MP2	1.0450	43.5549	0.9853	0.9351
MP3	1.0106	38.3631	1.0150	0.9784
MP4	1.2163	42.0205	1.1494	1.1049

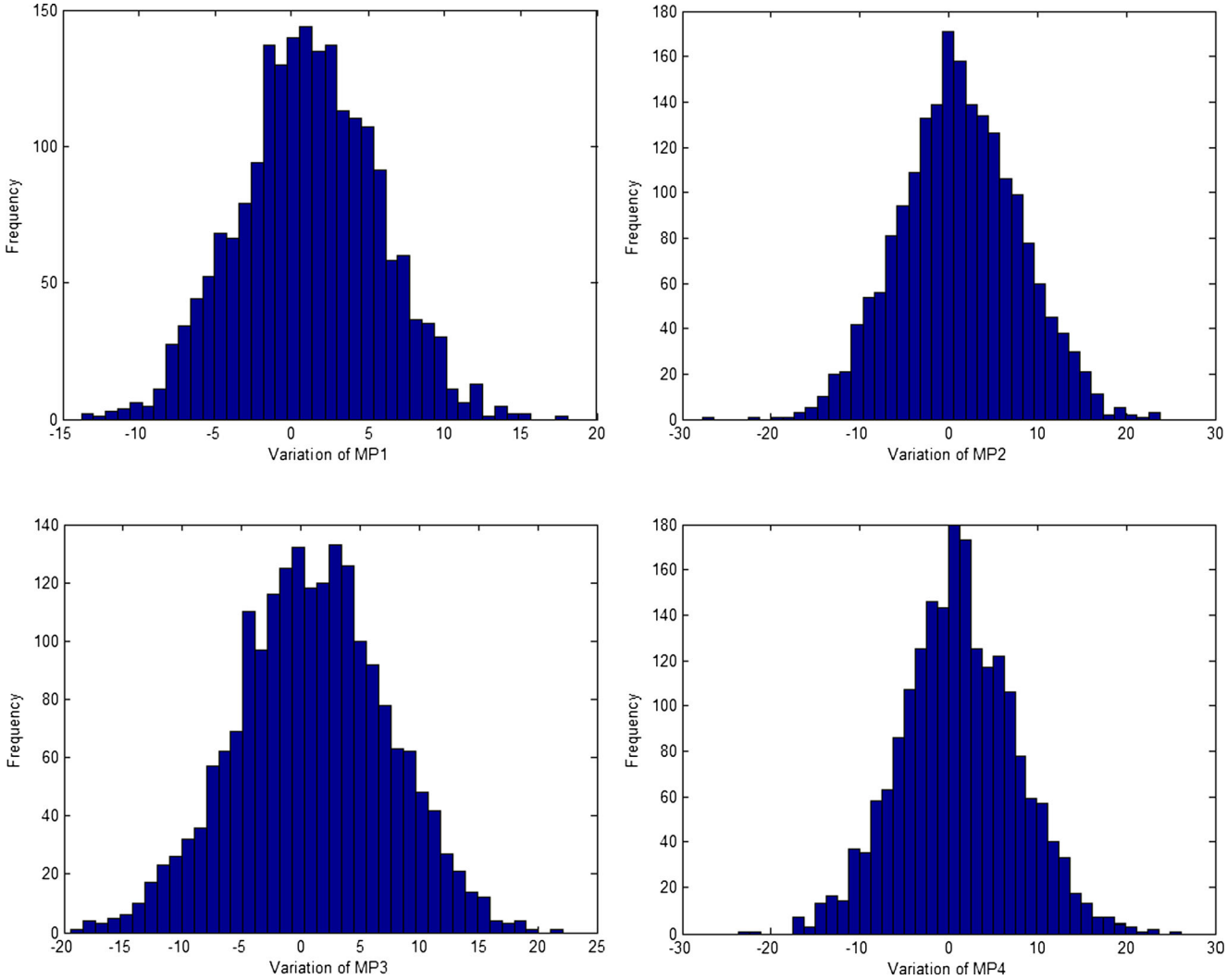

Fig. 24 Histogram of the variation of key points

6 Conclusions

This paper presents a study of the variation analysis and prediction of fuselage panel riveting assembly. The MIC based on key features is proposed, and riveting deformation computation method is developed and validated. Based on the case studies presented, the following statements can be made:

1. The part deformation along the riveting seam could be seen as the result of an equivalent exterior moment. This standpoint has been known as an experience in aircraft factory. By analyzing the deformation mechanism of the riveting process, the calculation method of assembly variation caused by riveting deformation is developed and validated. The method avoided the time-consuming elastic-plastic riveting process analysis and so enhanced the feasibility and the practicality of the riveting assembly variation prediction of fuselage panel.
2. Conventionally, the MIC established a linear relationship between the deviation input at variational points and the deviation output at key characteristic points [23]. On one hand, there may be dependencies between the variations at different points on the same sheet metal part (e.g., points on the same face may have proportioned deviation). On the other hand, the huge number of variational points causes difficulty in CAD or CAE modeling. Obviously, the traditional MIC could not deal with these two problems well. The MIC based on key features is proposed, and the traditional one is called as the MIC based on points for distinction. The MIC based on key features effectively solves the problems, and so it is more suitable for variation analysis in aircraft assembly.

Actually, the above analysis also shows that assembly variation in any state, such as joints or conformal tooling mounted, measurement before the next assembly station, can

be computed according to the boundary conditions. And also, the variation can be used as the prerequisite conditions of variation computation of the next station assembly.

As a final note, it should be emphasized that the present method only predicts the riveting assembly variation approximately, and since there are variances of riveting processes, the applicability of the method needs to be checked.

Acknowledgments This work is supported by the National Natural Science Foundation of China (GrantNo.51305395), National Natural Science Foundation of China (GrantNo.51275463), and Science Fund for Creative Research Groups of National Natural Science Foundation of China (NO. 51221004).

References

1. Ceglarek D, Huang W, Zhou S, Ding Y, Kumar R, Zhou Y (2009) Time-based competition in multistage manufacturing: stream-of-variation analysis (SOVA) methodology—review. J Flex Manuf Syst 16:11–44
2. Whitney DE, Gilbert OL, Jastrzebski M (1994) Representation of geometric variations using matrix transformation for statistical tolerance analysis in assembly. Res Eng Des 6:191–210
3. Huang W, Lin J, Bezdecny M, Kong Z, Ceglarek D (2007) Stream-of-variation modeling—part I: a generic 3D variation model for rigid body assembly in single station assembly processes. ASME J Manuf Sci Eng 129:821–831
4. Huang W, Lin J, Kong Z, Ceglarek D (2007) Stream-of-variation modeling—part II: a generic 3D variation model for rigid body assembly in multi station assembly processes. ASME J Manuf Sci Eng 129:832–842
5. Liu CS, Hu SJ (1997) Variation simulation for deformable sheet metal assemblies using finite element methods. ASME J Manuf Sci Eng 199:368–374
6. Cai W, Hsieh C, Long Y, Marin SP, Oh KP (2006) Digital panel assembly methodologies and application for compliant sheet components. ASME J Manuf Sci Eng 128(1):270–279
7. Xie K, Wells L, Camelio JA, Youn BD (2007) Variation propagation analysis on compliant assemblies considering contact interaction. ASME J Manuf Sci Eng 129(5):934–942
8. Liao X, Wang GG (2007) Non-linear dimensional variation analysis for sheet metal assemblies by contact modeling. Finite Elem Anal Des 44:34–44
9. Dahlstrom S, Lindkvist L (2007) Variation simulation of sheet metal assemblies using the method of influence coefficients with contact modeling. ASME J Manuf Sci Eng 129(3):615–622
10. Ungemach G, Mantwill F (2009) Efficient consideration of contact in compliant assembly variation analysis. ASME J Manuf Sci Eng 131:1–7
11. Ceglarek, D, and Shi, J (1997) Tolerance analysis for sheet metal assembly using a beam-based model. Proceeding concurrent product design and environmentally conscious manufacturing, Dallas, TX. November.
12. Li B, Tang H, Yang XP, Wang H (2006) Quality design of fixture planning for sheet metal assembly. Int J Adv Manuf Technol. doi:10.1007/S00170-005-0385-2
13. Camelio JA (2002) Modeling and diagnosis of dimensional variation for assembly systems with compliant part, Ph.D. Dissertation. University of Wisconsin, Madison
14. Phoomboplab T, Ceglarek D (2008) Process yield improvement through optimum design of fixture layouts in 3d multistation assembly systems. Trans ASME J Manuf Sci Eng 130:1–17
15. Camelio JA, Hu JS, Marin SP (2004) Compliant assembly variation analysis using component geometric covariance. J Manuf Sci Eng 126:355–360
16. Yue J, Camelio JA, Chin M, Cai W (2006) Product-oriented sensitivity analysis for multistation compliant assemblies. Trans ASME J Mech Des 129:844–851
17. Merkley K (1998) Tolerance analysis of compliant assemblies. PhD Thesis, Brigham Young University
18. Camelio J, Heichelbech B (2006) Comparison of diagnosis methods in sheet metal assembly. Trans NAMRI 34:135–142
19. Cai W (2008) A new tolerance modeling and analysis methodology through a two-step linearization with applications in automotive body assembly. SME J Manuf Syst 27:26–35
20. Cai W (2006) Robust pin layout design for sheet metal locating. Int J Adv Manuf Technol 28:486–494
21. Cai W, Hu SJ, Yuan JX (1996) Deformable sheet metal fixturing: principles, algorithms and simulations. ASME J Mech Des 118(3): 318–324
22. Cai W, Wang PC, Yang W (2005) Assembly dimensional prediction for self-piercing riveted aluminum panels. Int J Mach Tools Manuf 45:695–704
23. Moos S, Vezzetti E, Zompi A (2011) Assembly analysis for spot-welded compliant assembly: guidelines for formalizing the plasticity contribution to tolerance analysis. Proceedings of the IMProVe, International Conference on Innovative Methods in Product Design, June 15th–17th , Venice, Italy
24. Eckert A, Israel M, Neugebaner R, Rössinger M, Wahl M, Schulz F (2013) Local–global approach using experimental and/or simulated data to predict distortion caused by mechanical joining technologies. Prod Eng 7:339–349
25. Chang M, Gossard DC (1997) Modeling the assembly of compliant non-ideal parts. Comput Aided Des 29:701–708
26. Liu SC, Hu S (1997) Variation simulation for deformable sheet metal assemblies using finite element methods. ASME J Manuf Sci Eng 119:368–374
27. Nepershin RI, Knigin VV (1992) Interferences and residual stresses in riveted joints. J Mach Manuf Reliab 5:47–51
28. Muller R P (1995) An experimental and analytical investigation on the fatigue behavior of fuselage riveted lap-joints. Ph.D. Dissertation, Dept. of Mechanical Engineering, Delft Univ. of Technology, Delft, The Netherlands.
29. Li G, Shi G, Bellinger NC (2005) Studies of residual stress in single-row countersunk riveted lap joints", 46th AIAA Structures, Structural Dynamics and Materials Conference. AIAA, Austin, pp 18–21, 2005–2024
30. Atre A (2006) A finite element and experimental investigation on the fatigue of riveted lap joints in aircraft., PhD Thesis, Georgia Institute of Technology, Atlanta, Georgia.
31. Rans CD (2007) The role of rivet installation on the fatigue performance of riveted lap joints. Ph.D. dissertation, Carleton University, Ottawa
32. Skorupa A, Skorupa M (2012) Riveted lap joints in aircraft fuselage, solid mechanics and its applications 189. Springer Sci Bus Media Dordrecht. doi:10.1007/978-94-007-4282-6
33. Abaqus Inc., ABAQUS theory manual 6.10, http://www.abaqus.com
34. Yarkovets AI, Sirotkin OS, Firsov VV, Kisilev NM (1987) Processes for ensuring long life of riveted and bolted joints in aircraft structures. Mashinostroyeniye, Moscow
35. Demina NI, Volkov A K (1989) The influence of the interference of a rivet on the mechanical properties of D16 alloy sheet in biaxial tension, Cambridge science abstracts, aluminum industry abstracts, accession No. 01901145–0483,3:407–409
36. Hearn EJ (1997) Mechanics of materials 2, 3rd edn. Butterworth-Heinemann, Oxford
37. Franciosa P, Patalano S (2011) Simulation of variational compliant assemblies with shape errors based on morphing mesh approach. Int J Adv Manuf Technol 53:47–61